SUPPORTING INFORMATION

Correlated patterns of genetic diversity and differentiation across an avian family

Benjamin M. Van Doren, Leonardo Campagna, Barbara Helm, Juan Carlos Illera, Irby J. Lovette, and Miriam Liedvogel

ADDITIONAL METHODS

Draft Reference Genome

To extract DNA from Siberian stonechat (*S. maurus*) muscle tissue, we used the Gentra Puregene Tissue kit, following the protocol for fixed tissue. Gel electrophoresis revealed the DNA to be composed of highly intact molecules (all visible >10 kb). The ALLPATHS-LG algorithm (Gnerre et al. 2011) used 90.1% of the fragment library (total 506,475,396 reads), covering the genome at a mean depth of 46.9x. Combined, the two mate-pair libraries comprised 923,232,904 reads; ALLPATHS-a used 20.7% of these reads, which covered the genome at 19.6x. This initial assembly required 147.50 hours on a 64-core computer with 512 GB of memory (1735.37 hours of CPU time). ALLPATHS-LG grouped 39,301 contigs into 4,396 scaffolds, with a total scaffold length of 1.027 Gb. The N50 scaffold size was 8.02 Mb, and 4.6% of bases were ambiguous (N's).

We then used HaploMerger (Huang et al. 2012) to improve the assembly by merging homologous contigs and removing those that had arisen from the erroneous split of two haplotypes. HaploMerger requires "soft-masking" repetitive elements in the genome, which we did with RepeatMasker version open-4.0.2 (Smit et al. 2013-2015). HaploMerger has been used to improve a number of genome assemblies in this manner (e.g., Derks et al. 2015; Davey et al. 2016). After running the original assembly through the Haplomerger pipeline using default settings (and manually breaking two scaffolds that HaploMerger indicated may have been misjoined), the final Siberian stonechat *de novo* assembly comprised 2,819 scaffolds, with a total scaffold length of 1.020 Gb; the N50 scaffold size increased to 10.0 Mb compared to the original assembly. We verified that the majority of removed scaffolds had fragment library coverage of less than 5x. Haplomerger therefore appears to have been successful in removing a large number of small scaffolds that likely represented duplicates (i.e., heterozygous regions). The 1,577 removed scaffolds spanned only 7.4 Mb (0.7% of the original assembly).

To assess completeness of the reference genome, we used NCBI command-line 'blastn' to search for 5561 ultraconserved elements identified by Faircloth et al. (2012) from an analysis of chicken, anole, and zebra finch. The final assembly contained 5486 (98.7%) of these ultraconserved elements. Because they are interspersed throughout the entire genome, this percentage can be considered an approximation for the completeness of the draft assembly; a value of 98.7% is evidence that the assembly covers nearly the entire Siberian stonechat genome.

Sampling

Most birds used in this study originated from the common-garden stonechat study that Eberhard Gwinner initiated in 1981 at the Max-Planck Institute in Andechs, Germany.

Specifically, parental populations originated from the following locations: Austrian stonechats from Lower Austria (48°14’N, 16°22’E); Irish stonechats from Iveragh Peninsula near Killarney, in the County of Kerry, Ireland (c. 52°N, 10°W); African stonechats from Lake Nakuru region, Kenya (0°14’S, 36°0’E), and Mount Meru region, Tanzania (3°50’S, 36°5’E); and Siberian stonechats from the vicinity of Naursum National Park (c. 51.5°N, 63°E), Kazakhstan. All blood samples for the Canary Islands stonechat were collected directly in the field between 2013 and 2016 at various locations on Fuerteventura, Canary Islands, Spain (Barranco de Mal Nombre, Fimbapaire, Norte de Fenimoy, Barranco de Jacomar, Barranco Gran Valle, Barranco de Los Canarios, Barranco de Vinamar).

Pooled sequencing

We selected between 49 and 56 individuals (including both males and females) from each stonechat taxon based on a careful assessment of DNA quantity via Trinean DropSense 96 multi-channel spectrophotometer (Trinean, Ghent, Belgium) and quality (check for integrity on a 2% agarose gel), and we created one library of pooled DNA for each taxon following the Illumina TruSeq DNA kit. Each library included an equimolar aliquot of DNA from each individual. We multiplexed 4 of the 5 five groups on one lane of an Illumina NextSeq sequencer (151-bp paired end reads), and ran the fifth with three unrelated samples on a second lane. Thus, each group was sequenced on approximately one-fourth of a lane.

We demultiplexed raw sequence data from the sequencer with the ‘bcl2fastq’ utility by Illumina, using default settings. This utility generates ‘.fastq’ files after removing reads showing a 10% or greater error rate in the adapter sequence or more than 1 error in the barcode. It also masks adapter sequences extending into reads. We then used the program ‘skewer’ to conduct the following additional quality control measures on reads: trim the 3’ end until quality ≥ 20 is reached; and remove reads with normalized error rate > 0.1 (default), indel error rate > 0.03 (default, based on comparison with known adapter sequence), mean base quality < 20, or >15% ambiguous bases (N’s). Approximately 1% of the demultiplexed reads failed these criteria and were removed.

We used BWA-MEM (Li 2013) to align the pooled sequences to the reference genome, marking shorter split hits as secondary. We then converted the alignments to compressed BAM format using ‘samtools view,’ specifying a minimum mapping quality of 20. We sorted BAM files with ‘samtools sort’ and merged them across lanes using Picard’s ‘MergeSamFiles’ (Picard: http://broadinstitute.github.io/picard/). Following this, we marked duplicate reads using Picard’s MarkDuplicates utility; performed local realignment using the Genome Analysis Toolkit (GATK; RealignerTargetCreator and IndelRealigner) (McKenna et al. 2010; DePristo et al. 2011); and fixed mate information in Picard (FixMateInformation). Finally, we took the resulting 5 BAM files (one per taxon) and used ‘samtools mpileup’ to construct an mpileup file comparing the bases in overlapping reads at each position of the genome across populations.

Mapping quality for all stonechat taxa was high (Table S2). Mean mapping quality was lower for *Ficedula* species (*hypoleuca*: 35.64; *albicollis*: 35.82), but a high proportion of reads from these species were successfully mapped to the stonechat reference genome (*hypoleuca*: 0.93; *albicollis*: 0.95). This high mapping rate suggests that we are not introducing substantial bias by aligning flycatcher reads to the stonechat reference genome. We detected bacterial DNA contamination in some of the stonechat pools; these sequences did not map to the reference and were thereafter ignored.

Mapping to *Ficedula* chromosomes

We assembled scaffolds from the stonechat assembly into draft chromosomes by mapping them to the *Ficedula albicollis* genome assembly, version 1.5 (RefSeq accession GCF_000247815.1; http://www.ncbi.nlm.nih.gov/assembly/GCF_000247815.1; http://www.ncbi.nlm.nih.gov/genome/?term=txid59894[orgn]) (Kawakami et al. 2014). We used SatsumaSynteny (Grabherr et al. 2010) to align the *Saxicola* draft genome to the *F. albicollis* assembly. This method unambiguously placed nearly all scaffolds of sufficient size (> 10 Kb) on a *F. albicollis* chromosome, with 85% of scaffolds mapping to single chromosomes across >70% of their extents. In the rare cases (~1%) where scaffolds mapped to more than one *Ficedula* chromosome across greater than 20% the scaffold length, we assigned the scaffold to the chromosome with the greatest amount of sequence aligned (always a majority of the scaffold). SatsumaSynteny thus allowed us to position scaffolds from the stonechat genome in the correct order and orientation along the chromosomes, assuming that synteny is conserved in these taxa (Ellegren 2013). This assumption appears robust given the high conservation of sequence within scaffolds. SatsumaSynteny successfully mapped 97.1% of the stonechat reference genome to a *Ficedula* chromosome. Most unmapped scaffolds had not passed the 10 Kb threshold.

Coverage heterogeneity

To rule out the possibility that variation in coverage could be driving differentiation patterns, we compared read depth in F_{ST} outlier regions to read depth outside of those regions. We selected the comparison of Irish and Siberian stonechats because this comparison showed arguably the most conspicuous F_{ST} peaks, and therefore any effect of coverage should be most pronounced. Because allele frequencies in adjacent 50 Kb windows are autocorrelated due to linkage and therefore contribute to pseudoreplication, we subsampled the genome at a ratio of 1:10. We used *t*-tests to test for differences inside and outside of outlier regions. Read depth was not significantly different within and outside of F_{ST} peaks for both taxa (Irish: $t = 0.78$, df = 118.37, $P = 0.44$; Siberian: $t = 0.89$, df = 119.56, $P = 0.39$). Specifically, for Irish stonechats, mean within-peak coverage was 26.01 and mean outside-of-peak coverage was 26.38. For Siberian stonechats these values were 15.08 and 15.23, respectively.

Phylogeny

We aligned raw reads from Pied and Collared Flycatcher re-sequencing data to the stonechat genome in order to call genotypes. We then selected 17,527,493 sites across the genome which satisfied the following criteria: minimum coverage of 5 in all populations; fixation of a single allele at the locus (allowing a maximum count of 1 of another allele because of the possibility for sequencing error); and variation in the fixed allele among the 7 taxa. Using these SNPs, we generated a phylogenetic tree with RAxML v. 8.2.6 (Stamatakis 2014) on CIPRES (http://www.phylo.org). We applied the Lewis correction, following the recommendation of Stamatakis (2014), for ascertainment bias resulting from the exclusion of constant sites and using 100 bootstrapped replicates to assess branch support.

Choice of window size and bandwidth size for genome-wide scans

We used a window size of 50 Kb for our genomic analyses because it provided us sufficiently fine resolution across the genome while still averaging over hundreds of SNPs per window. We felt it was important not to rely heavily on allele frequencies of individual SNPs because of the random variation in allele frequencies introduced by our pooled sequencing approach. We conducted a sensitivity analysis (not shown) and found that we identified fewer and larger outlier regions as we increased window size, but that the level of overlap detected between genomic landscapes did not systematically vary. We feel that this justifies a window size of 50 Kb because it allows us to capture relatively small outlier regions while keeping the number of regions to a manageable size for this whole-genome analysis of multiple taxa.

We selected a bandwidth of 30 because it allowed us to identify relatively small regions of differentiation while still providing a benefit by smoothing out apparent noise in the data. We conducted a sensitivity analysis (not shown) and found that the median size of outlier regions identified by our analysis stayed relatively constant until a bandwidth of about 50, after which we observed an increase. Therefore, we do not believe that we are biased towards detecting large outlier regions by using a bandwidth of 30. We also did not observe any systematic effect of bandwidth size on the level of overlap detected between genomic landscapes.

SUPPLEMENTARY FIGURES

Figure S1. Boxplots comparing F_{ST} and π between the Z chromosome and autosomes. Outlier values are not shown. Under neutral expectation, the equilibrium level of neutral variability is proportional to the effective population size, and the effective population size of the Z chromosome is expected to be three-fourths that of the autosomes because females only have one copy (Charlesworth 2001). We used a *t*-test for ratios (*t.test.ratio* function in the *mratios* package) to test whether the ratio of π on the Z chromosome to π on the autosomes was significantly different from 0.75 (Djira et al. 2012). Stonechats and flycatchers showed π ratios between 0.74-0.83; Kenyan, Siberian and Canary Islands stonechats and Pied Flycatchers (*Ficedula hypoleuca*) had π ratios that did not significantly differ from 0.75, while Austrian and Irish stonechats and Collared Flycatchers (*Ficedula albicollis*) showed slightly more diverse Z chromosomes than expected by theory. In all cases, F_{ST} on the Z chromosome was elevated over that of the autosomes, with ratios in stonechats between 1.04-1.29, and a much higher ratio in flycatchers of 1.80.

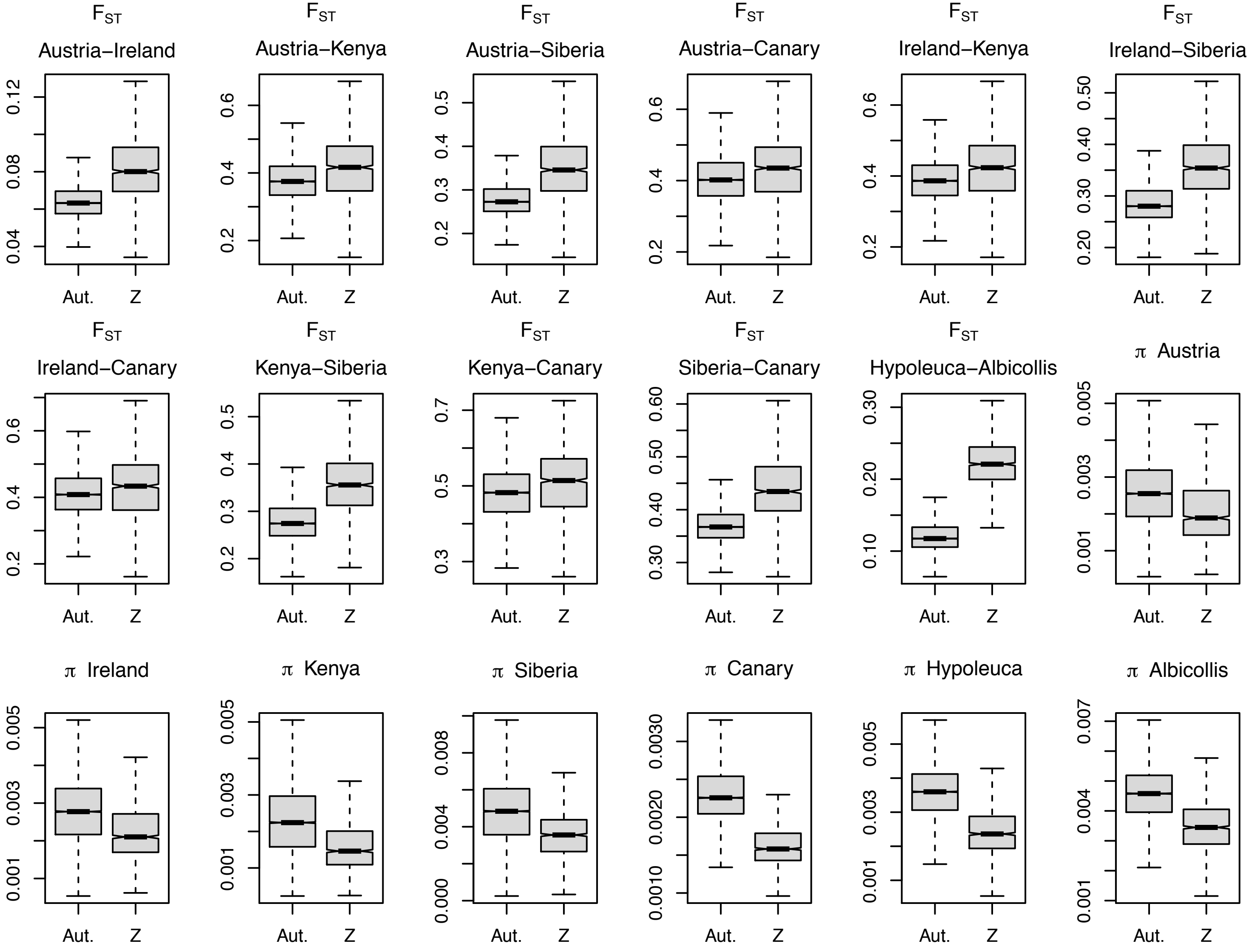
F_{ST}
Austria–Ireland
0.04
0.08
0.12
Aut.
Z
F_{ST}
Austria–Kenya
0.2
0.4
0.6
Aut.
Z
F_{ST}
Austria–Siberia
0.2
0.3
0.4
0.5
Aut.
Z
F_{ST}
Austria–Canary
0.2
0.4
0.6
Aut.
Z
F_{ST}
Ireland–Kenya
0.2
0.4
0.6
Aut.
Z
F_{ST}
Ireland–Siberia
0.20
0.30
0.40
0.50
Aut.
Z
F_{ST}
Ireland–Canary
0.2
0.4
0.6
Aut.
Z
F_{ST}
Kenya–Siberia
0.2
0.3
0.4
0.5
Aut.
Z
F_{ST}
Kenya–Canary
0.3
0.5
0.7
Aut.
Z
F_{ST}
Siberia–Canary
0.30
0.40
0.50
0.60
Aut.
Z
F_{ST}
Hypoleuca–Albicollis
0.10
0.20
0.30
Aut.
Z
π Austria
0.001
0.003
0.005
Aut.
Z
π Ireland
0.001
0.003
0.005
Aut.
Z
π Kenya
0.001
0.003
0.005
Aut.
Z
π Siberia
0.000
0.004
0.008
Aut.
Z
π Canary
0.0010
0.0020
0.0030
Aut.
Z
π Hypoleuca
0.001
0.003
0.005
Aut.
Z
π Albicollis
0.001
0.004
0.007
Aut.
Z

Figure S2. Genome-wide landscape of d_{XY} for pairwise comparisons of stonechats and Pied and Collared Flycatchers (*Ficedula albicollis* and *F. hypoleuca*). All stonechat comparisons showed very similar genomic landscapes of d_{XY}. Many outlier regions were also shared with *Ficedula*, especially on the larger chromosomes. For clarity, comparisons including Irish stonechats are not included (with the exception of Austria-Ireland), because of the high degree of similarity between Austrian and Irish taxa. The colored lines are kernel-based density smoothers. Individual points represent 50-Kb windows; scaffolds alternate dark gray and light gray coloring. Chromosomes (based on alignment to *Ficedula albicollis*) are delineated by thick dark gray or light gray lines on the upper border of each plot and are labeled above this line. Z* indicates a flycatcher Z chromosome linkage group that could not be exactly placed in the flycatcher genome assembly. Shaded orange rectangles show d_{XY} peaks and blue rectangles show d_{XY} valleys.

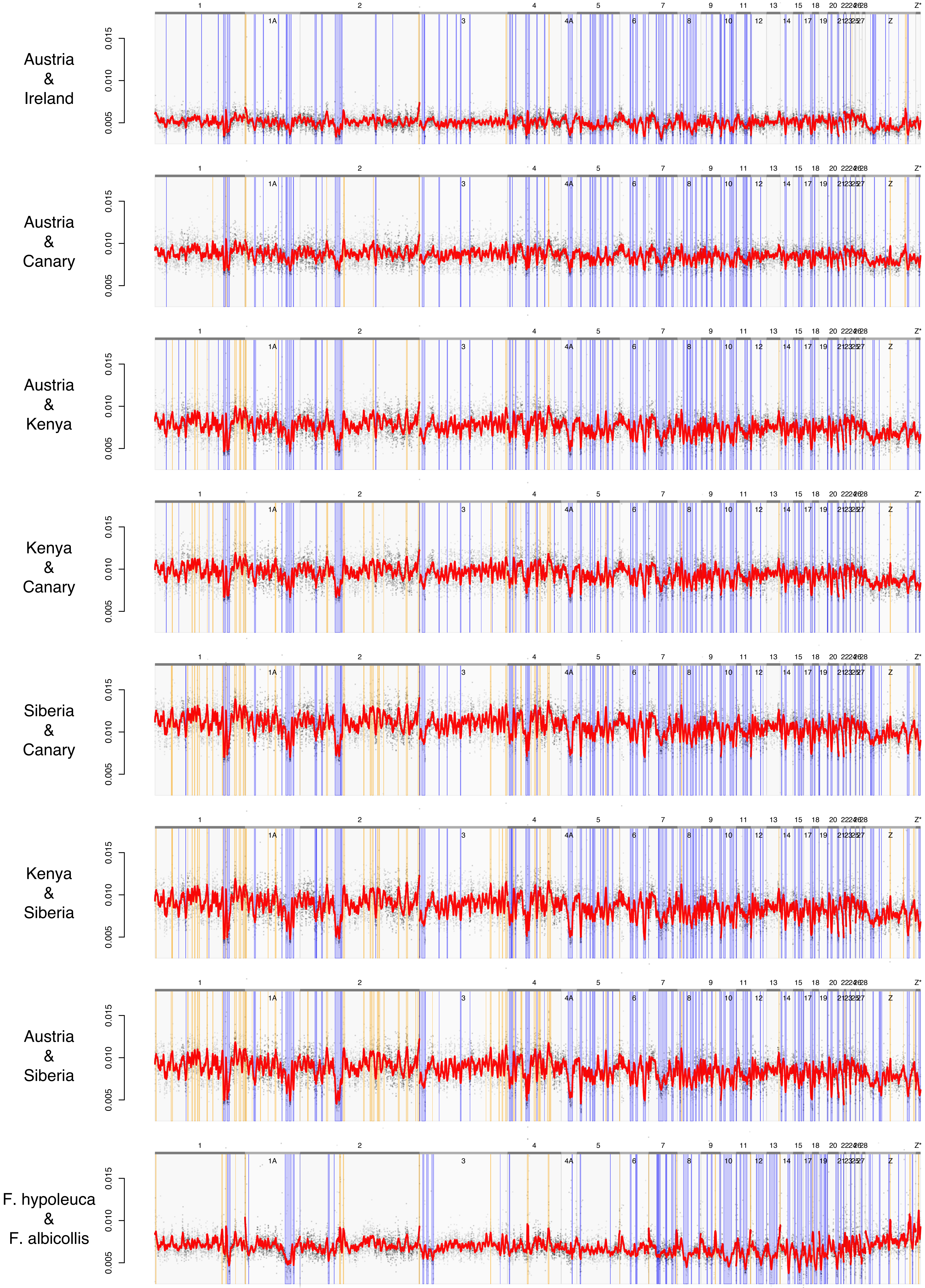
Austria & Ireland
Austria & Canary
Austria & Kenya
Kenya & Canary
Siberia & Canary
Kenya & Siberia
Austria & Siberia
F. hypoleuca & F. albicollis
0.005
0.010
0.015
1
1A
2
3
4
4A
5
6
7
8
9
10
11
12
13
14
15
17
18
19
20
21
22
23
24
25
26
27
28
Z
Z*

Figure S3. D_{XY} across stonechat chromosome 1A. All stonechat comparisons show very similar fluctuations, including two pronounced valleys. The largest valley is also apparent in the comparisons of Pied and Collared Flycatchers (*Ficedula albicollis* and *F. hypoleuca*). Blue rectangles indicate significant d_{XY} valleys. See Figure S2 for other details. For clarity, comparisons including Irish stonechats are not included (with the exception of Austria-Ireland) because of the high degree of similarity between Austrian and Irish populations.

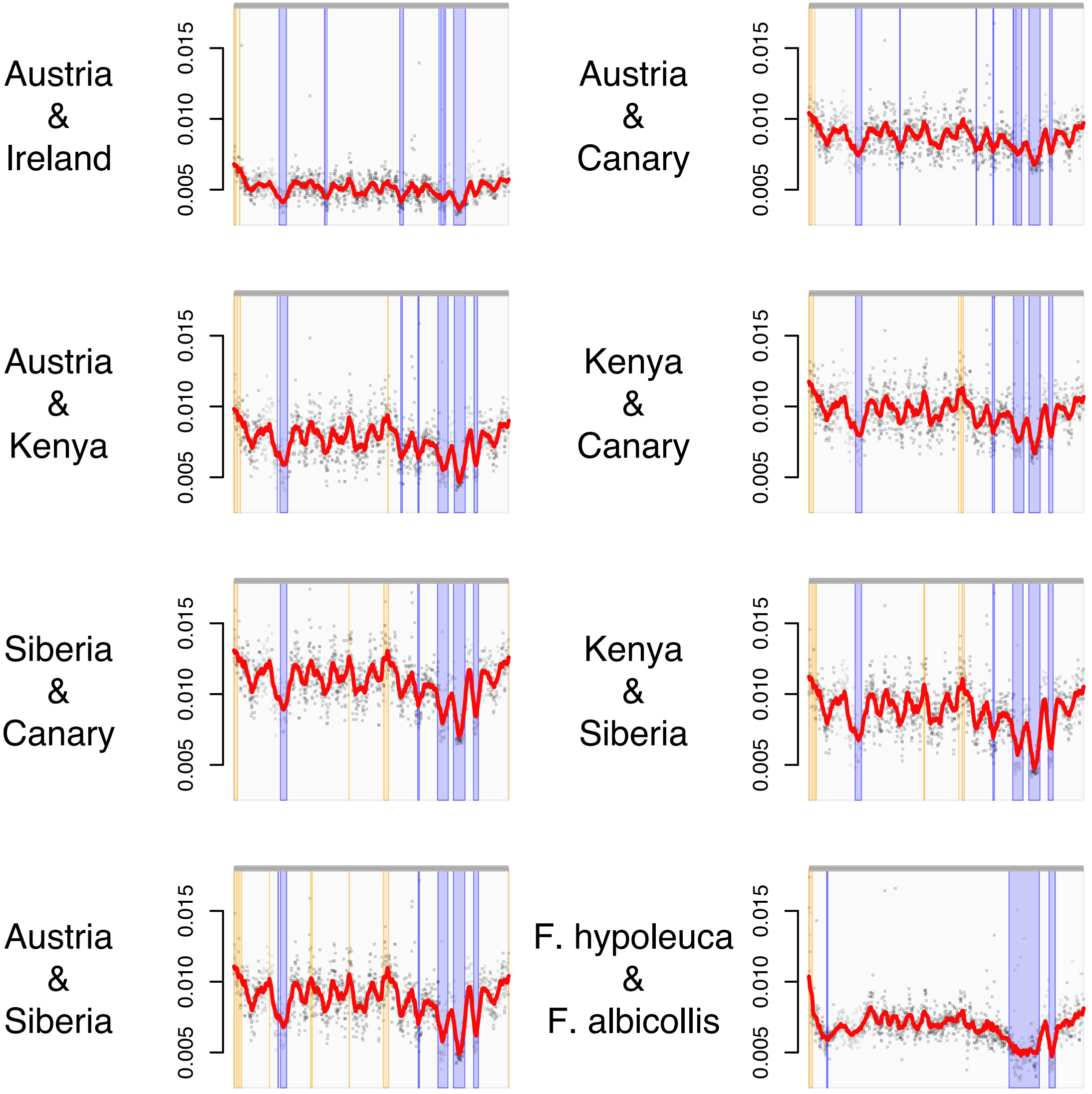
Austria & Ireland
Austria & Canary
Austria & Kenya
Kenya & Canary
Siberia & Canary
Kenya & Siberia
Austria & Siberia
F. hypoleuca & F. albicollis
0.005
0.010
0.015

Figure S4. Correlation of high d_{XY} regions among stonechats and flycatchers (*Ficedula hypoleuca* and *albicollis*, or “Hyp.” and “Alb.”). Matrix shows outlier similarity scores, which quantify the number of high-d_{XY} “peaks” shared among different comparisons. Some comparisons including Irish stonechats are not shown because of their similarity to Austrian stonechats. All tests were significant after applying a false discovery rate correction. Cells with yellow backgrounds indicate that four independent taxa are being compared.

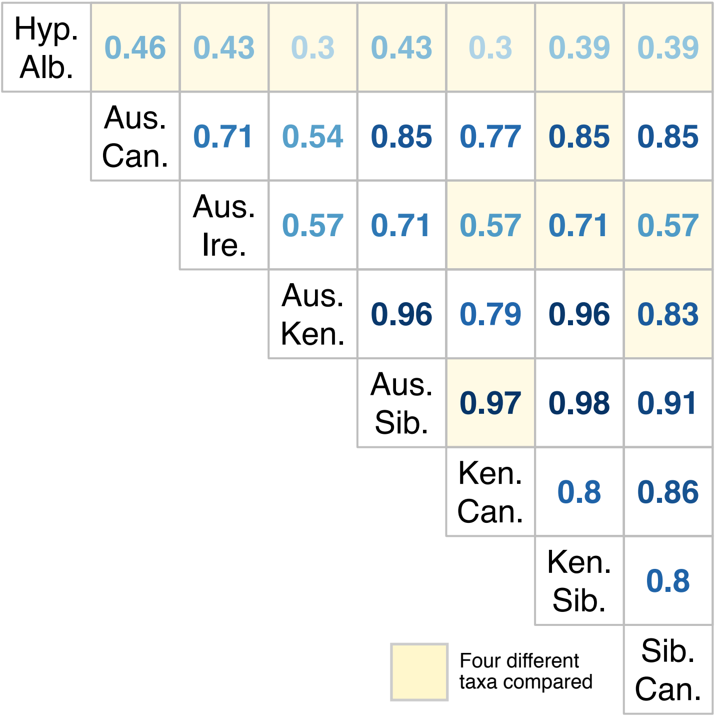

Hyp. Alb.	0.46 🟨	0.43 🟨	0.3 🟨	0.43 🟨	0.3 🟨	0.39 🟨	0.39 🟨
	Aus. Can.	0.71	0.54	0.85	0.77	0.85 🟨	0.85
		Aus. Ire.	0.57	0.71	0.57 🟨	0.71 🟨	0.57 🟨
			Aus. Ken.	0.96	0.79	0.96	0.83 🟨
				Aus. Sib.	0.97 🟨	0.98	0.91
					Ken. Can.	0.8	0.86
						Ken. Sib.	0.8
							Sib. Can.

🟨 Four different taxa compared

Figure S5. Genome-wide landscape of F_{ST} for pairwise comparisons of stonechats and Pied and Collared Flycatchers (*Ficedula albicollis* and *F. hypoleuca*). Pairs including Siberian stonechats showed the most conspicuous peaks; other comparisons showed less distinct outlier regions. Some comparisons (e.g., Kenya-Canary Is.) showed F_{ST} valleys in the same regions as the F_{ST} peaks of other comparisons. Shaded orange rectangles show F_{ST} peaks and blue rectangles show F_{ST} valleys. See Figure S2 for other details.

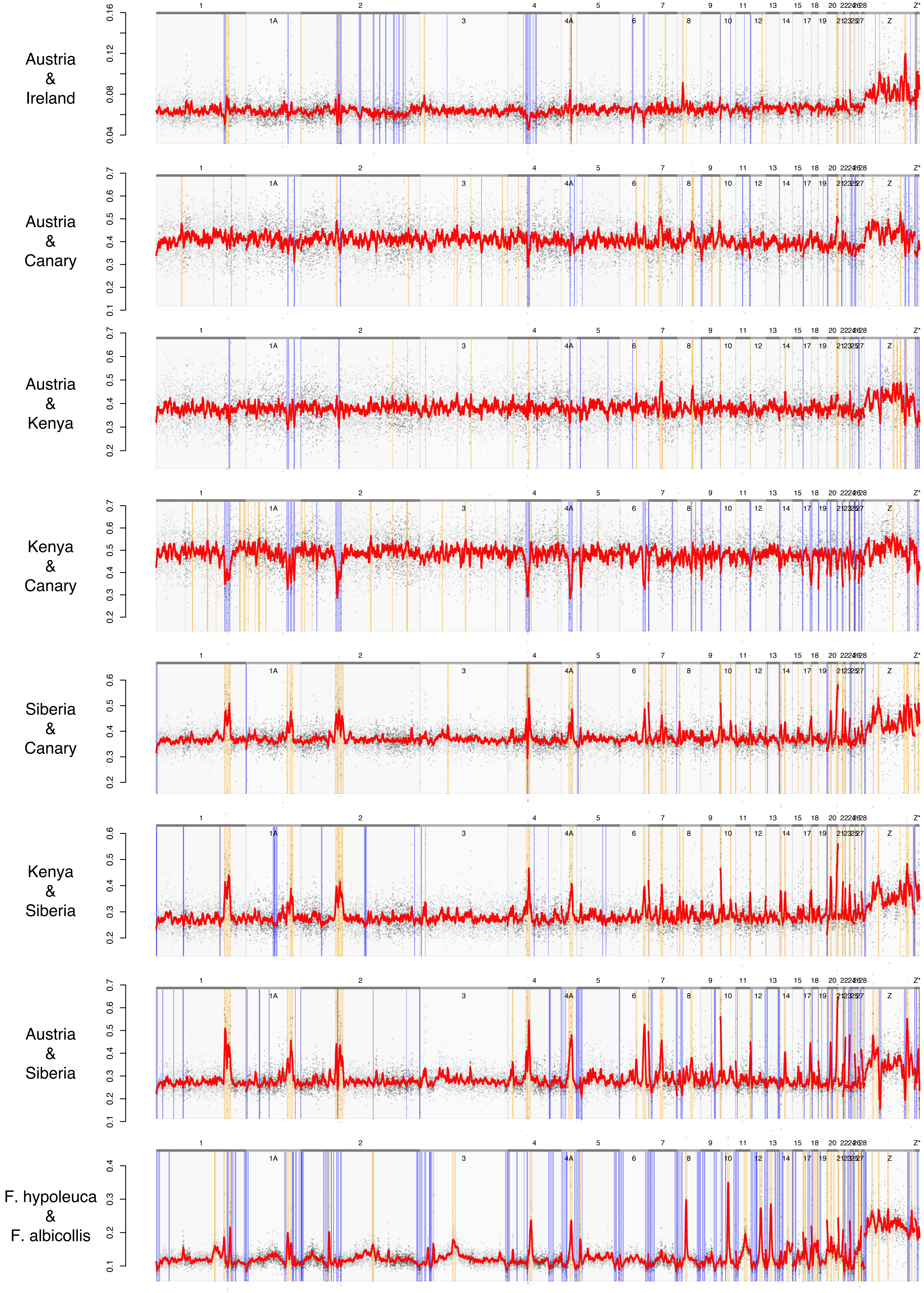
Austria & Ireland
0.04
0.08
0.12
0.16
Austria & Canary
0.1
0.2
0.3
0.4
0.5
0.6
0.7
Austria & Kenya
0.2
0.3
0.4
0.5
0.6
0.7
Kenya & Canary
0.2
0.3
0.4
0.5
0.6
0.7
Siberia & Canary
0.2
0.3
0.4
0.5
0.6
Kenya & Siberia
0.2
0.3
0.4
0.5
0.6
Austria & Siberia
0.1
0.2
0.3
0.4
0.5
0.6
0.7
F. hypoleuca & F. albicollis
0.1
0.2
0.3
0.4
1
2
4
5
7
9
11
13
15
18
20
22
24
26
28
Z*
1A
3
4A
6
8
10
12
14
17
19
21
23
25
27
Z

Figure S6. Genome-wide landscape of π for five stonechat taxa. Canary Islands stonechats generally did not share the valleys present in the genomes of the other taxa. See Fig. S2 for other details.

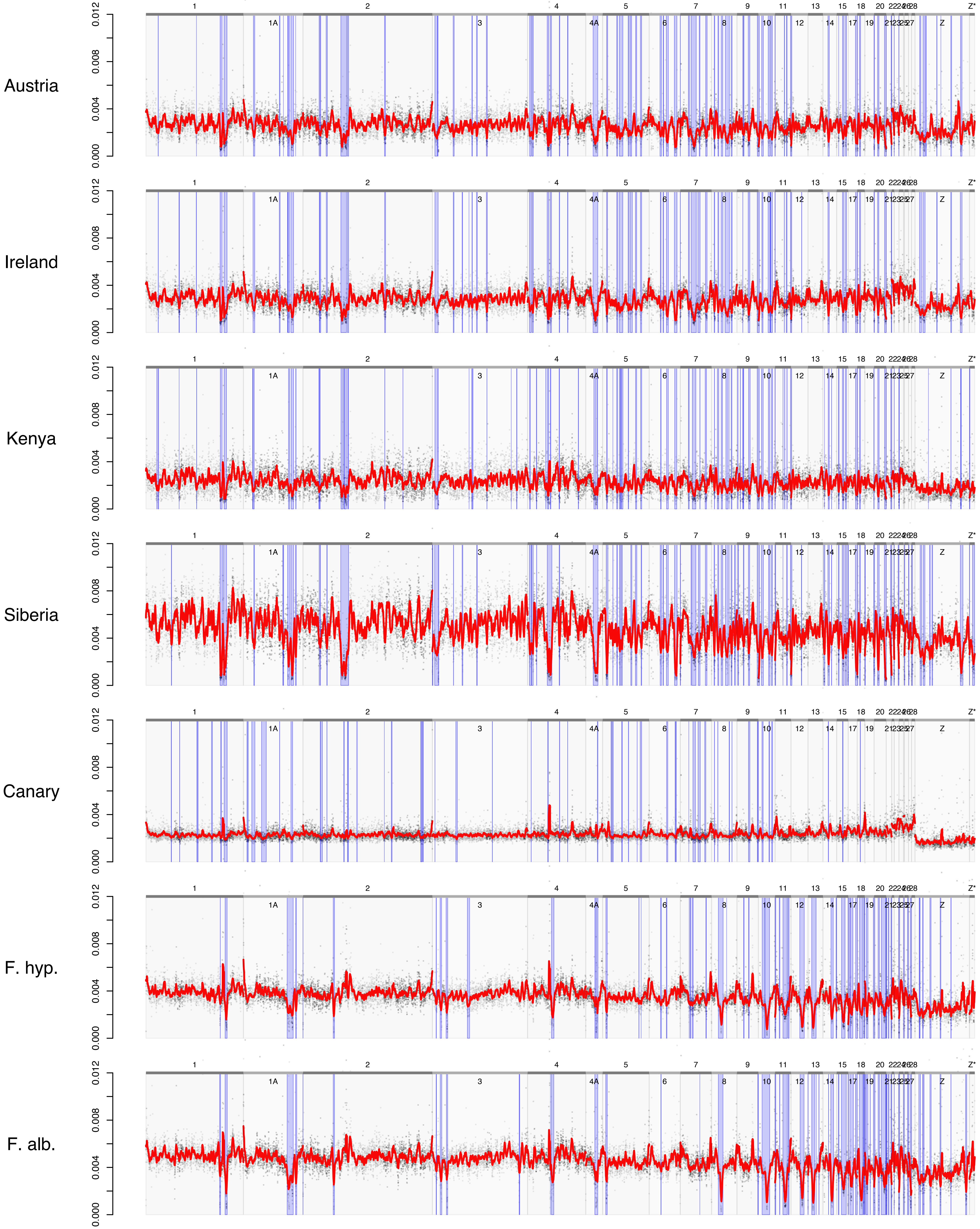
Austria
Ireland
Kenya
Siberia
Canary
F. hyp.
F. alb.
0.000
0.004
0.008
0.012
1
1A
2
3
4
4A
5
6
7
8
9
10
11
12
13
14
15
17
18
19
20
21
22
23
24
25
26
27
28
Z
Z*

Figure S7. Genome-wide landscape of standardized nucleotide diversity (π/d_{XY}) for five stonechat and two flycatcher taxa. Canary Islands stonechats did not share the valleys present in the genomes of the other taxa. See Fig. S2 for other details.

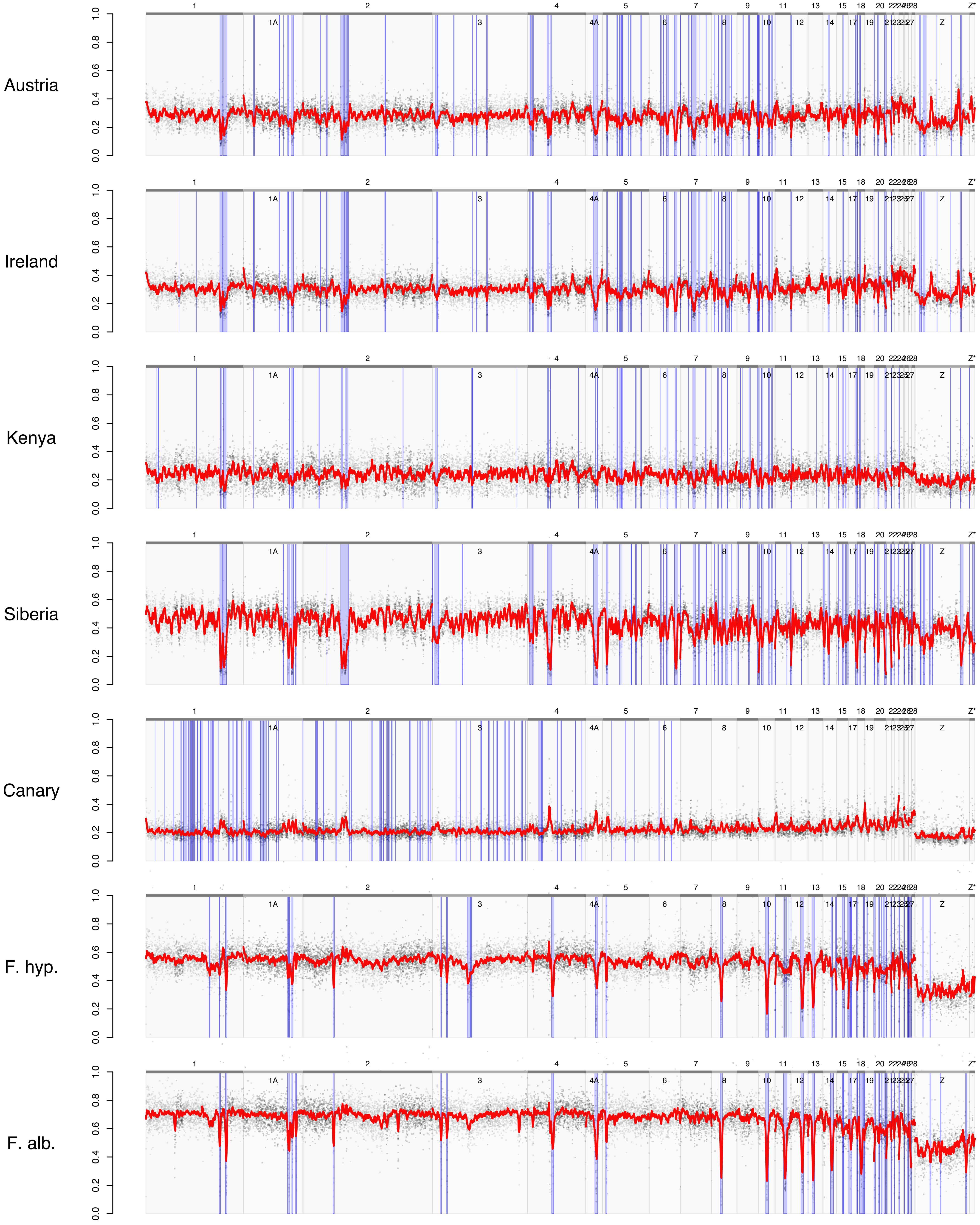
Austria
Ireland
Kenya
Siberia
Canary
F. hyp.
F. alb.
0.0
0.2
0.4
0.6
0.8
1.0
1
1A
2
3
4
4A
5
6
7
8
9
10
11
12
13
14
15
17
18
19
20
21
22
23
24
25
26
27
28
Z
Z*

Figure S8. Correlation of nucleotide diversity (π) with Tajima's *D* and Fay & Wu's *H* stonechats. Shown are outlier similarity scores, which quantify the number of low Fay & Wu's *H* "valleys" that coincide with low π (top section) and low Tajima's *D* (bottom section). Refer to Figs. 2-3 for details.

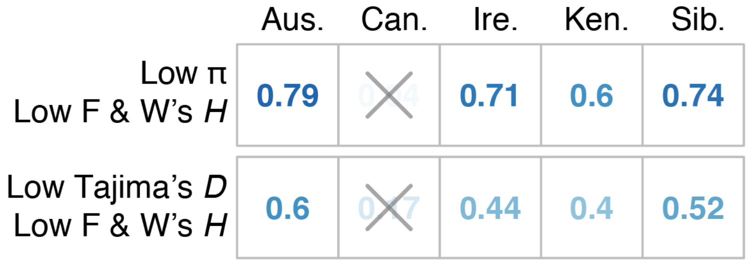

	Aus.	Can.	Ire.	Ken.	Sib.
Low π Low F & W's *H*	0.79	✗ 0.04	0.71	0.6	0.74
Low Tajima's *D* Low F & W's *H*	0.6	✗ 0.17	0.44	0.4	0.52

Figure S9. Genome-wide landscape of Tajima's *D* for five stonechat and two flycatcher taxa. Austrian, Irish, Siberian, and Kenyan stonechats shared similar genomic landscapes of Tajima's *D*. Canary Islands stonechats showed a different pattern, with very low Tajima's *D* across the entire genome. See Fig. S2 for other details.

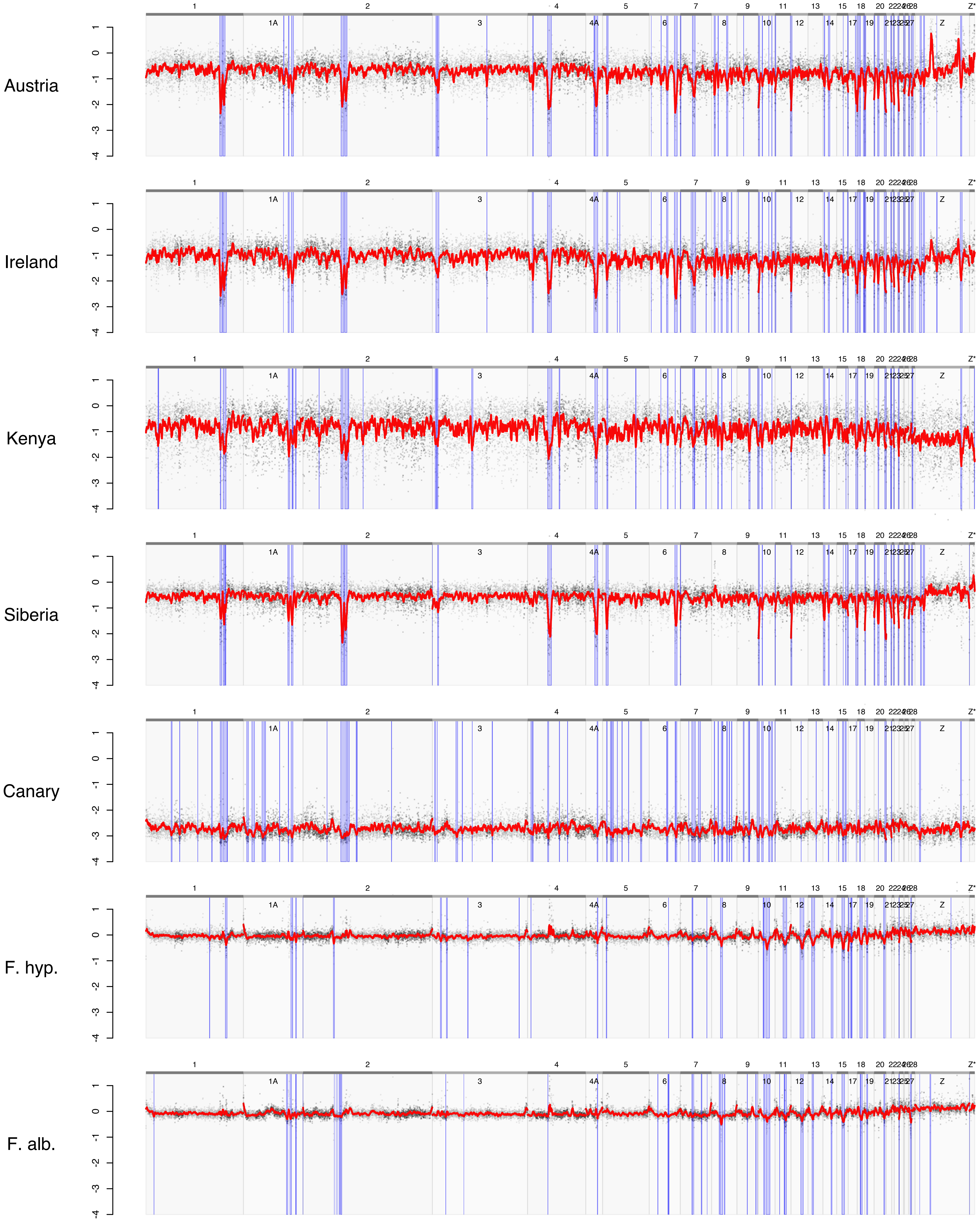
Austria
Ireland
Kenya
Siberia
Canary
F. hyp.
F. alb.
1
1A
2
3
4
4A
5
6
7
8
9
10
11
12
13
14
15
17
18
19
20
21
22
23
24
25
26
27
28
Z
Z*
1
0
-1
-2
-3
-4

Figure S10. Genomic landscape of Fay and Wu’s *H* for each of five stonechat taxa. See Fig. S2 for other details.

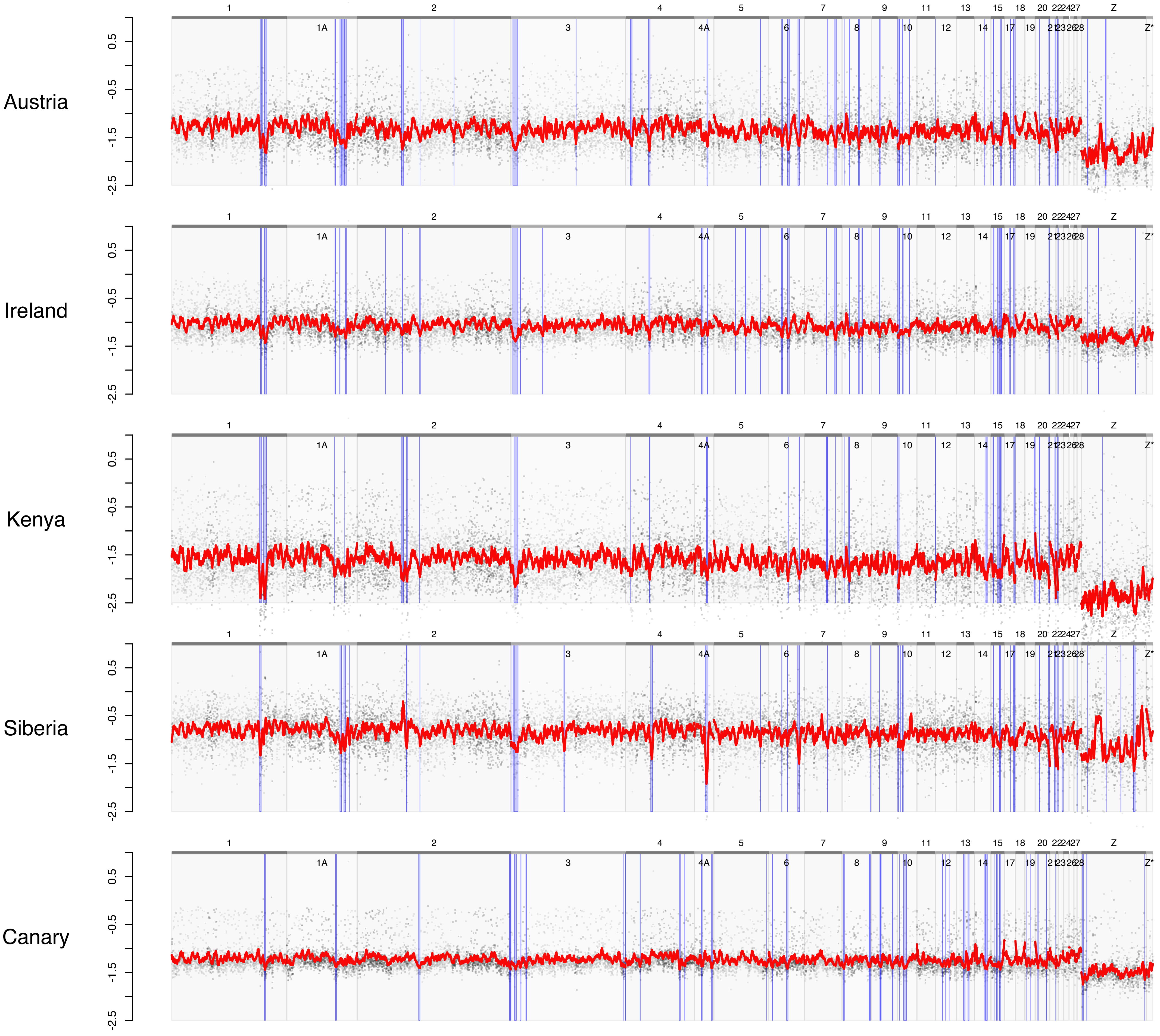
Austria
Ireland
Kenya
Siberia
Canary
1
1A
2
3
4
4A
5
6
7
8
9
10
11
12
13
14
15
17
18
19
20
21
22
23
24
26
27
28
Z
Z*
0.5
-0.5
-1.5
-2.5

Figure S11. F_{ST} across stonechat chromosome 13, including Pied and Collared Flycatchers (*Ficedula albicollis* and *F. hypoleuca*). The *Ficedula* comparison shows a distinct peak, which is not present in any stonechat comparison. This suggests that the evolutionary processes driving differentiation in this chromosome are potentially unique to *Ficedula*. See Fig. S2 for other details.

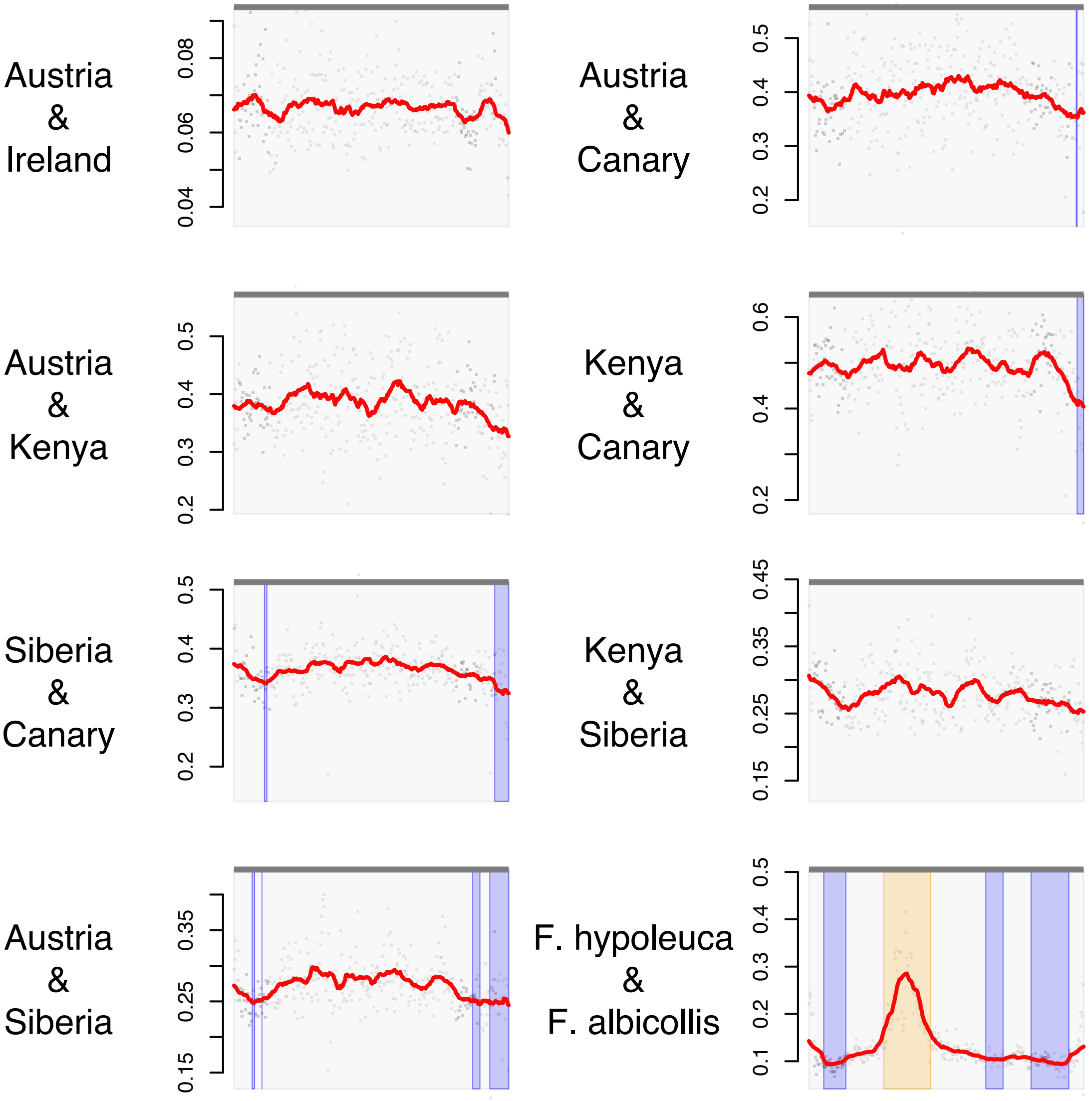
Austria & Ireland
0.04
0.06
0.08
Austria & Canary
0.2
0.3
0.4
0.5
Austria & Kenya
0.2
0.3
0.4
0.5
Kenya & Canary
0.2
0.4
0.6
Siberia & Canary
0.2
0.3
0.4
0.5
Kenya & Siberia
0.15
0.25
0.35
0.45
Austria & Siberia
0.15
0.25
0.35
F. hypoleuca & F. albicollis
0.1
0.2
0.3
0.4
0.5

Figure S12. F_{ST} across stonechat chromosome 20, including Pied and Collared Flycatchers (*Ficedula albicollis* and *F. hypoleuca*). Comparisons including the Siberian population show a distinct peak at the right end of the chromosome. Notably, this peak is absent in *Ficedula*, suggesting that the evolutionary processes driving divergence in this chromosome are potentially unique to the stonechat radiation. Also note that the Kenya-Canary comparison shows a valley in the center of the chromosome, where there is a peak in other comparisons. See Fig. S2 for other details.

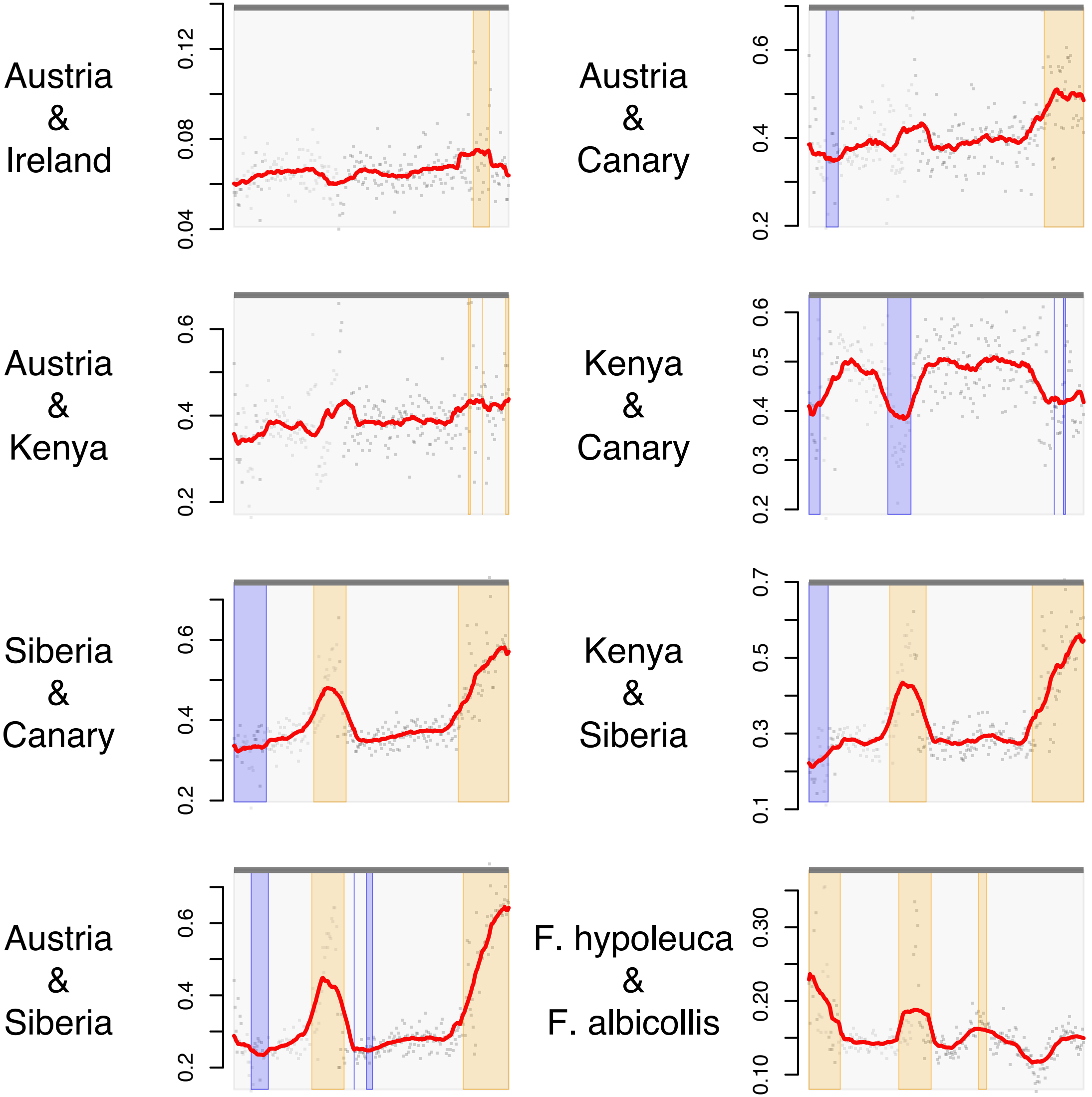
Austria & Ireland
0.04
0.08
0.12
Austria & Canary
0.2
0.4
0.6
Austria & Kenya
0.2
0.4
0.6
Kenya & Canary
0.2
0.3
0.4
0.5
0.6
Siberia & Canary
0.2
0.4
0.6
Kenya & Siberia
0.1
0.3
0.5
0.7
Austria & Siberia
0.2
0.4
0.6
F. hypoleuca & F. albicollis
0.10
0.20
0.30

Figure S13. F_{ST} across stonechat chromosome 4A, including Pied and Collared Flycatchers (*Ficedula albicollis* and *F. hypoleuca*). Comparisons including Siberian stonechats, *Ficedula*, and Austria-Ireland show a distinct peak. The other comparisons show a valley in the same region. See Fig. S2 for other details.

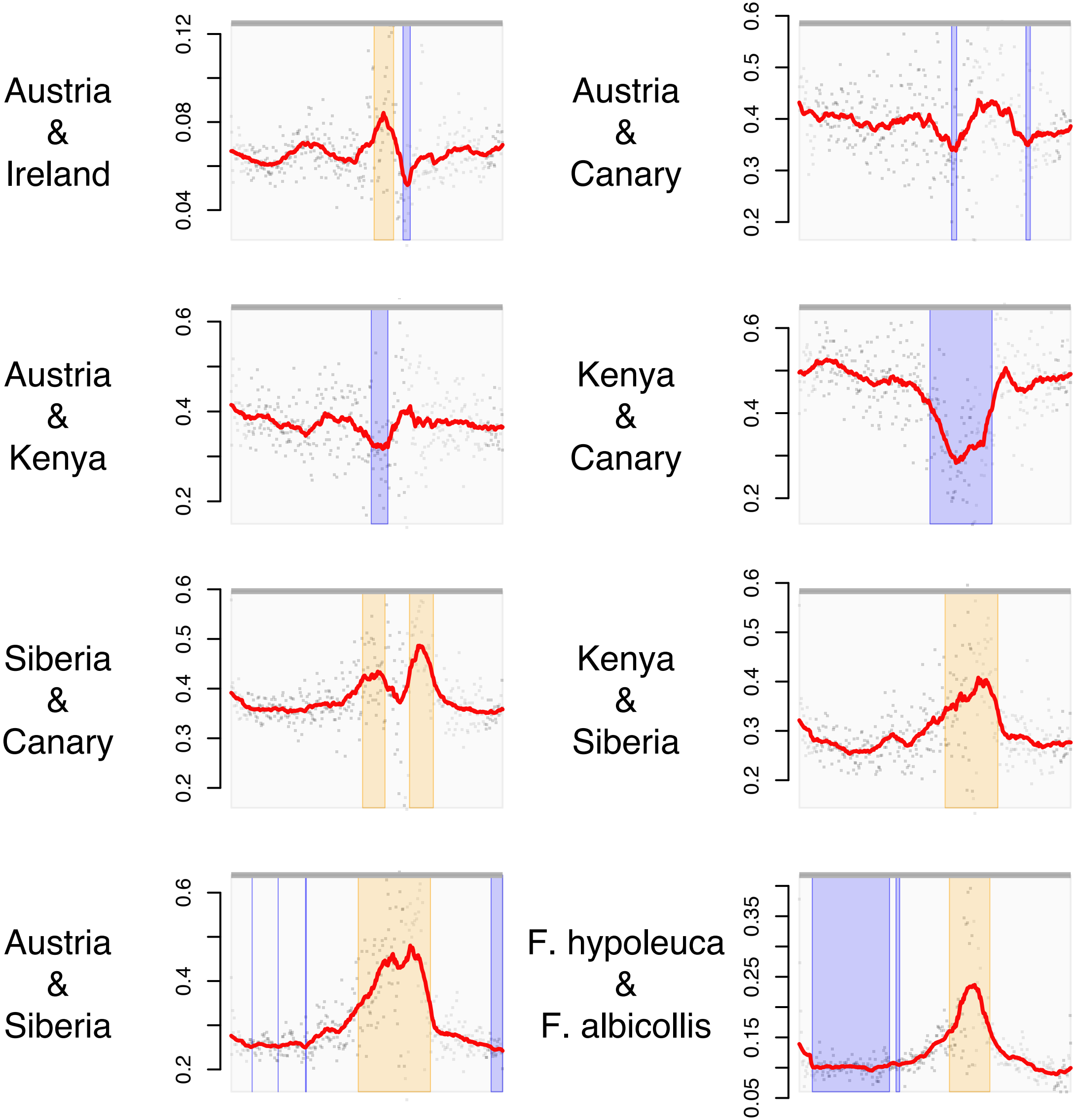
Austria & Ireland
0.04
0.08
0.12
Austria & Canary
0.2
0.3
0.4
0.5
0.6
Austria & Kenya
0.2
0.4
0.6
Kenya & Canary
0.2
0.4
0.6
Siberia & Canary
0.2
0.3
0.4
0.5
0.6
Kenya & Siberia
0.2
0.3
0.4
0.5
0.6
Austria & Siberia
0.2
0.4
0.6
F. hypoleuca & F. albicollis
0.05
0.15
0.25
0.35

Figure S14. F_{ST} across stonechat chromosome 1A, including Pied and Collared Flycatchers (*Ficedula albicollis* and *F. hypoleuca*). Comparisons including Siberian stonechats and *Ficedula* show a distinct peak. Other comparisons show a valley in the same region. See Fig. S2 for other details.

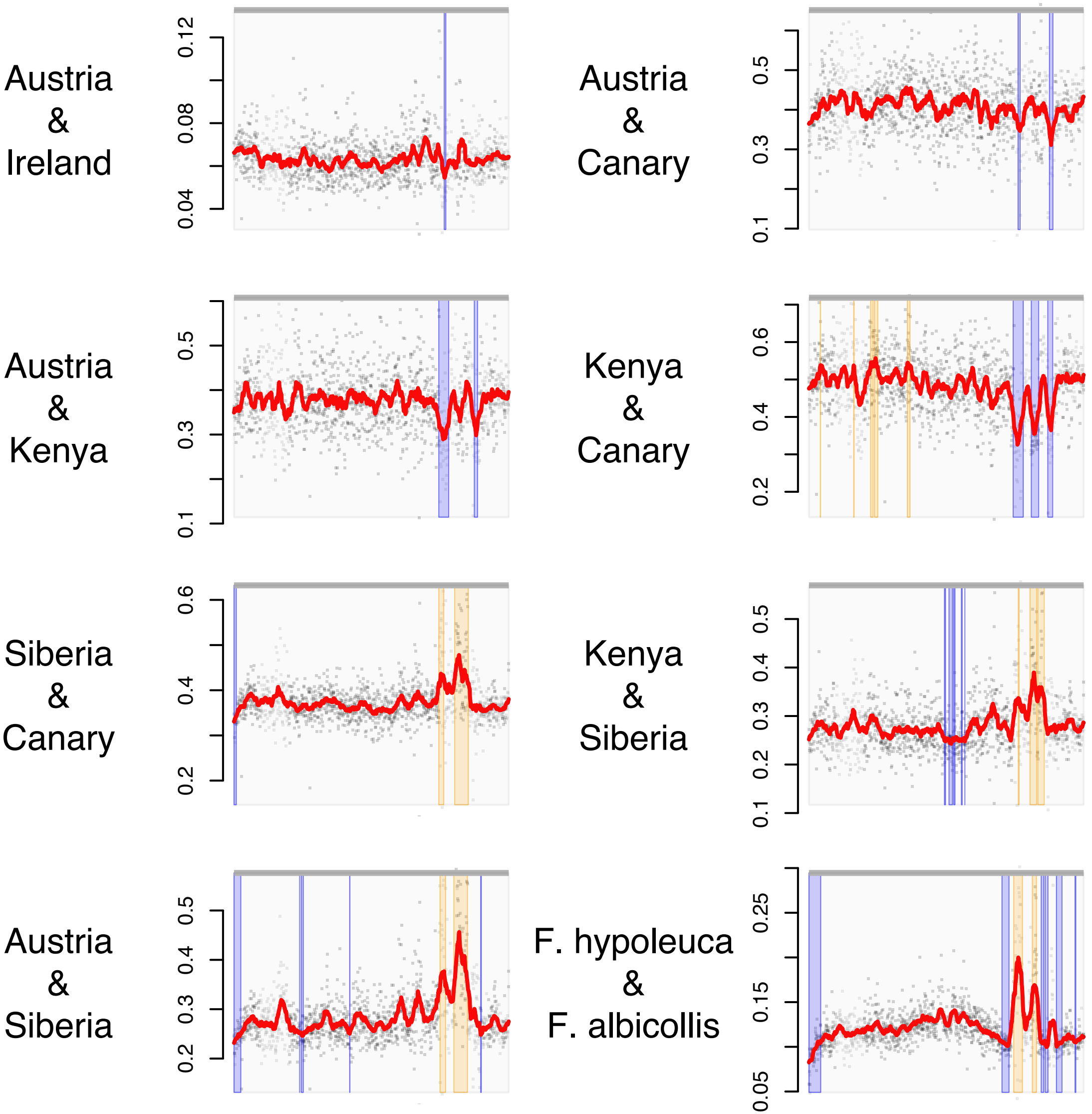
Austria & Ireland
0.04
0.08
0.12
Austria & Canary
0.1
0.3
0.5
Austria & Kenya
0.1
0.3
0.5
Kenya & Canary
0.2
0.4
0.6
Siberia & Canary
0.2
0.4
0.6
Kenya & Siberia
0.1
0.2
0.3
0.4
0.5
Austria & Siberia
0.2
0.3
0.4
0.5
F. hypoleuca & F. albicollis
0.05
0.15
0.25

SUPPLEMENTARY TABLES

Table S1. Origin, sex, and relatedness information of stonechats included in this study. Kinship matrices were calculated with the *kinship* function in the R package *kinship2* (Therneau and Sinnwell 2015) using a pedigree of captive stonechats, and values presented are the mean (+SD) values from each kinship matrix. Inbreeding coefficients were calculated with the *calcInbreeding* function in the R package *pedigree* (Coster 2013). IQR stands for interquartile range.

	Origins		Sex		Relatedness					
	Direct from wild	Hatched in captivity	Male	Female	Mean kinship	SD kinship	Median kinship	IQR kinship	Mean inbreeding	SD inbreeding
Austria	1	48	27	22	0.014	0.045	0	0	0.006	0.018
Ireland	27	27	26	28	0.009	0.043	0	0	0.002	0.012
Kenya	1	50	18	33	0.009	0.039	0	0	0.012	0.05
Siberia	0	52	30	22	0.033	0.064	0	0.0625	0.005	0.017
Canary	56	0	38	18	-	-	-	-	-	-

Table S2. Summary of alignment of Illumina 150-bp reads from five stonechat taxa to the draft reference genome. Mapping quality is given after filtering out alignments with a mapping quality of 20 or lower.

Taxon	Reads Mapped	Mean (Median) Coverage	Mean Mapping Quality
Kenya	98,758,285	13.8 (12.7)	45.61
Ireland	185,976,416	26.1 (24.8)	45.26
Austria	135,110,173	18.8 (17.7)	45.14
Siberia	107,623,583	14.9 (13.9)	45.80
Canary Islands	176,167,216	24.7 (23.9)	45.64

Table S3. *Ficedula* individuals included in the study (data from the Sequence Read Archive, or SRA, project ERP007074, published in Smeds et al. (2015)).

Species	SRA Run	Mean coverage of *Ficedula albicollis* genome
F. hypoleuca	ERR637490	16x
	ERR637491	12x
	ERR637492	11x
	ERR637493	11x
	ERR637494	13x
	ERR637495	16x
	ERR637496	18x
	ERR637501	14x
	ERR637503	14x
	ERR637504	12x
F. albicollis	ERR637505	14x
	ERR637506	14x
	ERR637508	10x
	ERR637511	16x
	ERR637512	15x
	ERR637513	14x
	ERR637515	11x
	ERR637519	12x
	ERR637522	11x
	ERR637523	13x

SUPPLEMENTARY REFERENCES

Charlesworth, B. 2001. The effect of life-history and mode of inheritance on neutral genetic variability. Genetics Research 77:153-166.

Coster, A. 2013. pedigree: Pedigree functions. R package version 1.4.

Davey, J. W., M. Chouteau, S. L. Barker, L. Maroja, S. W. Baxter, F. Simpson, M. Joron, J. Mallet, K. K. Dasmahapatra, and C. D. Jiggins. 2016. Major Improvements to the Heliconius melpomene Genome Assembly Used to Confirm 10 Chromosome Fusion Events in 6 Million Years of Butterfly Evolution. G3: Genes|Genomes|Genetics.

DePristo, M. A., E. Banks, R. Poplin, K. V. Garimella, J. R. Maguire, C. Hartl, A. A. Philippakis, G. del Angel, M. A. Rivas, M. Hanna, A. McKenna, T. J. Fennell, A. M. Kernytsky, A. Y. Sivachenko, K. Cibulskis, S. B. Gabriel, D. Altshuler, and M. J. Daly. 2011. A framework for variation discovery and genotyping using next-generation DNA sequencing data. Nat Genet 43:491-498.

Derks, M. F. L., S. Smit, L. Salis, E. Schijlen, A. Bossers, C. Mateman, A. S. Pijl, D. de Ridder, M. A. M. Groenen, M. E. Visser, and H.-J. Megens. 2015. The Genome of Winter Moth (*Operophtera brumata*) Provides a Genomic Perspective on Sexual Dimorphism and Phenology. Genome Biology and Evolution 7:2321-2332.

Djira, G. D., M. Hasler, D. Gerhard, and F. Schaarschmidt. 2012. mratios: Inferences for ratios of coefficients in the general linear model. R package version 1.3. 17.

Ellegren, H. 2013. The Evolutionary Genomics of Birds. Annual Review of Ecology, Evolution, and Systematics 44:239-259.

Faircloth, B. C., J. E. McCormack, N. G. Crawford, M. G. Harvey, R. T. Brumfield, and T. C. Glenn. 2012. Ultraconserved Elements Anchor Thousands of Genetic Markers Spanning Multiple Evolutionary Timescales. Systematic Biology.

Gnerre, S., I. MacCallum, D. Przybylski, F. J. Ribeiro, J. N. Burton, B. J. Walker, T. Sharpe, G. Hall, T. P. Shea, S. Sykes, A. M. Berlin, D. Aird, M. Costello, R. Daza, L. Williams, R. Nicol, A. Gnirke, C. Nusbaum, E. S. Lander, and D. B. Jaffe. 2011. High-quality draft assemblies of mammalian genomes from massively parallel sequence data. Proceedings of the National Academy of Sciences 108:1513-1518.

Grabherr, M. G., P. Russell, M. Meyer, E. Mauceli, J. Alföldi, F. Di Palma, and K. Lindblad-Toh. 2010. Genome-wide synteny through highly sensitive sequence alignment: Satsuma. Bioinformatics 26:1145-1151.

Huang, S., Z. Chen, G. Huang, T. Yu, P. Yang, J. Li, Y. Fu, S. Yuan, S. Chen, and A. Xu. 2012. HaploMerger: reconstructing allelic relationships for polymorphic diploid genome assemblies. Genome research 22:1581-1588.

Kawakami, T., L. Smeds, N. Backström, A. Husby, A. Qvarnström, C. F. Mugal, P. Olason, and H. Ellegren. 2014. A high-density linkage map enables a second-generation collared flycatcher genome assembly and reveals the patterns of avian recombination rate variation and chromosomal evolution. Molecular Ecology 23:4035-4058.

Knief, U. and W. Forstmeier. 2015. Mapping centromeres of microchromosomes in the zebra finch (*Taeniopygia guttata*) using half-tetrad analysis. Chromosoma:1-12.

Li, H. 2013. Aligning sequence reads, clone sequences and assembly contigs with BWA-MEM. arXiv preprint arXiv:1303.3997.

McKenna, A., M. Hanna, E. Banks, A. Sivachenko, K. Cibulskis, A. Kernytsky, K. Garimella, D. Altshuler, S. Gabriel, and M. Daly. 2010. The Genome Analysis Toolkit: a MapReduce framework for analyzing next-generation DNA sequencing data. Genome research 20:1297-1303.

Smeds, L., V. Warmuth, P. Bolivar, S. Uebbing, R. Burri, A. Suh, A. Nater, S. Bures, L. Z. Garamszegi, S. Hogner, J. Moreno, A. Qvarnstrom, M. Ruzic, S.-A. Saether, G.-P. Saetre, J. Torok, and H. Ellegren. 2015. Evolutionary analysis of the female-specific avian W chromosome. Nat Commun 6.

Smit, A., R. Hubley, and P. Green. 2013-2015. RepeatMasker Open-4.0.

Stamatakis, A. 2014. RAxML Version 8: A tool for Phylogenetic Analysis and Post-Analysis of Large Phylogenies. Bioinformatics.

Therneau, T. M. and J. Sinnwell. 2015. kinship2: Pedigree Functions. R package version 1.6.4.

Warren, W. C., D. F. Clayton, H. Ellegren, A. P. Arnold, L. W. Hillier, A. Kunstner, S. Searle, S. White, A. J. Vilella, S. Fairley, A. Heger, L. Kong, C. P. Ponting, E. D. Jarvis, C. V. Mello, P. Minx, P. Lovell, T. A. F. Velho, M. Ferris, C. N. Balakrishnan, S. Sinha, C. Blatti, S. E. London, Y. Li, Y.-C. Lin, J. George, J. Sweedler, B. Southey, P. Gunaratne, M. Watson, K. Nam, N. Backstrom, L. Smeds, B. Nabholz, Y. Itoh, O. Whitney, A. R. Pfenning, J. Howard, M. Volker, B. M. Skinner, D. K. Griffin, L. Ye, W. M. McLaren, P. Flicek, V. Quesada, G. Velasco, C. Lopez-Otin, X. S. Puente, T. Olender, D. Lancet, A. F. A. Smit, R. Hubley, M. K. Konkel, J. A. Walker, M. A. Batzer, W. Gu, D. D. Pollock, L. Chen, Z. Cheng, E. E. Eichler, J. Stapley, J. Slate, R. Ekblom, T. Birkhead, T. Burke, D. Burt, C. Scharff, I. Adam, H. Richard, M. Sultan, A. Soldatov, H. Lehrach, S. V. Edwards, S.-P. Yang, X. Li, T. Graves, L. Fulton, J. Nelson, A. Chinwalla, S. Hou, E. R. Mardis, and R. K. Wilson. 2010. The genome of a songbird. Nature 464:757-762.